Antimicrobial, Antioxidant, and Antiviral Activities of Biosynthesized Silver Nanoparticles by Phycobiliprotein Crude Extract of the Cyanobacteria *Spirulina platensis* and *Nostoc linckia*

Gehan A. Ismail[1] · Mostafa M. El-Sheekh[1] · Rehab M. Samy[1] · Saly F. Gheda[1]

Abstract

The present work was designed for the biosynthesis of silver nanoparticles (AgNPs) by *Spirulina platensis* and *Nostoc linckia* phycobiliprotein extract and for evaluation of their antimicrobial, antioxidant, and antiviral activities. The biosynthesized AgNPs were characterized by UV-Vis spectroscopy, Fourier transform-infrared spectroscopy, transmission electron microscopy, X-ray diffraction analysis, and Zeta potential analysis. The antimicrobial activity of the biosynthesized AgNPs was tested by the disk diffusion method. The antioxidant activity of the nanoparticles was assessed by using DPPH radical scavenging, total antioxidant capacity, and ferric reducing antioxidant assays. The antiviral activity of AgNPs was also challenged with the hepatitis C virus (HCV). The appearance of the surface plasmon resonance band at 420 nm indicated the biosynthesis of AgNPs. TEM images revealed that AgNPs had a mean average size of 21.211 and 21.052 nm for *S. platensis* and *N. linckia*, respectively. XRD analysis confirmed its spherical crystalline shape, and FTIR analysis suggested that proteins were responsible for their capping and stabilization. Zeta potential recorded − 15.902 mV and − 16.811 mV for *S. platensis* and *N. linckia* AgNPs, respectively, confirming its stability. AgNPs showed potent antimicrobial activity against some bacterial pathogens and *Candida albicans*. The antioxidant activity of AgNPs was evident by the use of three antioxidant assays. Significant antiviral activity against HCV (64.976%) was recorded for AgNPs of *N. linckia*, compared with Ribavirin (66.673%) as a standard drug, while *S. platensis* AgNPs recorded 48.334%. In conclusion, AgNPs biosynthesized from cyanobacterial phycobiliproteins were stable and showed potent antimicrobial, antioxidant, and antiviral activities.

Keywords Cyanobacteria · AgNPs · Zeta potential · RT-PCR · HCV

1 Introduction

Nanotechnology is an operation for the manufacture of materials ranged from 1 to 100 nm in size [1]. Nanoparticles display totally novel or enhanced characteristics, constructed on confident properties, like size, spreading, and morphology of the grains. Biological methods for nanoparticle synthesis using microorganisms [2–4], enzymes [5], and plant or plant extracts [6] have been suggested as possible eco-friendly alternatives to chemical and physical methods, which proved to be expensive and result in toxic byproducts [7]. They also have discrete physical, optical properties, and biochemical functionality due to diverse controlled size and shape [8].

Silver nanoparticles (AgNPs) have acquired increasing interest due to their unique physical properties, chemical reactivity, and potential applications as antimicrobial [9], anticancer [10], antioxidant [11], and antiviral [12]. The most widely known applications of AgNPs are in therapeutic manufacturing in medical device coatings, drug-delivery carriers, imaging probes, and implants of silver-impregnated polymers [13] to inhibit the occurrence of the infection. AgNPs are also the most effective in contradiction of bacteria, viruses, and other eukaryotic microorganisms among all metallic nanoparticles. This is mainly owing to the intrinsic inhibitory and bactericidal potential of silver, as well as due to their chemical stability, catalytic belongings, and dressed conductivity [14]. The antimicrobial activity of AgNPs synthesized via different biological approaches has been assessed against a wide range of multidrug-resistant bacterial and fungal pathogens. This includes Gram-negative bacteria such as *Pseudomonas*

✉ Mostafa M. El-Sheekh
mostafaelsheikh@science.tanta.edu.eg

1   Botany Department, Faculty of Science, Tanta University,
     Tanta 31527, Egypt

aeruginosa, *Klebsiella pneumoniae*, and *Escherichia coli* as well as Gram-positive bacteria such as *Staphylococcus aureus* [15]. In addition, AgNPs can also boost antifungal activity against numerous drug resistance fungal strains like *Aspergillus fumigatus*, *Fusarium solani*, *Aspergillus niger*, and *Aspergillus flavus* [16]. Presently, research tendencies are directed for screening and identifying new natural antioxidants from plant resources. Antioxidant activity in plant extracts is due to the redox potential of phytochemicals [6], which can play an important role in slaking singlet and triplet oxygen, disintegrating the peroxides, or neutralizing the free radicals. So, it is supposed that the favorite adsorption of an antioxidant component of a certain extract onto the surface of the nanoparticle is the main cause of the highest antioxidant activity of these nanoparticles [16]. The antioxidant activity of AgNPs proved by using many assays such as phosphomolybdenum assay, metal chelating activity, superoxide radical scavenging activity, DPPH radical scavenging activity, and ferric reducing/antioxidant power (FRAP) assays [17]. In a related context, AgNPs represent a novel class of antiviral agents due to their advantageous broad-spectrum antiviral activity [18, 19]; and because their antiviral action is occurring at non-cytotoxic concentrations compared to the current toxic broad-spectrum antivirals [20]. Singh et al. [14] mentioned a detailed review of the application of AgNPs as virucidal agents and demonstrated the effective inhibition of influenza viruses, which can be extended to other viruses as HIV, hepatitis C, and B viruses. The release of silver ions, cell membrane disruption, and DNA damage are the key mechanisms of AgNP action [18].

Basically, AgNP cytotoxicity is depending on their size and shape, capping or coating agent, concentration or dosage, surface charge, oxidation state, and the ability for agglomeration, as well as the pathogenic type for which AgNP toxicity is examined [21]. Numerous, in vitro, investigations have specified AgNP toxicity to mammalian cell lines, e.g., liver, lung, skin, and brain; the reproductive organs and vascular system cells as well [22]. However, a major concern of hazard practicing with respect to human health was prospected. In this context, a detailed review was conducted by Ferdous and Nemmar [23], who stated that AgNP toxicity and bio-distribution, in vivo, studies have proven Ag$^+$ translocation and accumulation leading to toxicity for different organs. The same review emphasized that complete characterization of NPs and proper control of assays are mandatory when applying AgNPs on humans and the environment [23].

Cyanobacteria, previously known as blue-green microalgae, have a noteworthy attraction as a natural source of bioactive compounds with a comprehensive range of biological activities counting antimicrobial, antiviral, anticancer, antioxidant, and antiinflammatory possessions [3, 24, 25]. Cyanobacteria are rich in phycobiliproteins (PBPs), the unique photosynthetic pigments of cyanobacteria [26].

Spirulina platensis and *Nostoc linckia* are two common cyanobacterial species, and phycobiliproteins extracted from them displayed favorable health benefits for improving immune function and inhibiting the proliferation of cancer cells due to their fluorescent properties [26]. These pigments have been broadly used in the fields of foods, pharmaceuticals, and cosmetics as a natural alternative for synthetic colorants [27]. Owing to their photosensitive ability, phycobiliproteins have been proposed as a novel photosensitizer for photodynamic therapy [28, 29]; in the field of immunology, in addition to their role as an antioxidant and antiinflammatory agents [30]. In light of the above-mentioned literature, the present study is conducted to extract phycobiliproteins from *S. platensis* and *N. linckia* cyanobacterial species. The ability of these pigments to act as a biological reductant for AgNP biosynthesis is evaluated. Also, the antimicrobial, antioxidant, and antiviral properties of these AgNPs were assessed for potent biological applications.

2 Materials and Methods

2.1 Cultivation of Cyanobacterial Species

Axenic cyanobacterial cultures were obtained from the culture collection of Phycology Laboratory, Botany Department, Faculty of Science, Tanta University. *Spirulina platensis* (Gomont) was cultivated in a modified Zarrouk medium [31], while *Nostoc linckia* (Bornet) was cultivated in a BG$_{11}$ medium [32]. For working cultures, 100 ml of stock inoculant corresponding to each species was cultured in 2-l Erlenmeyer flasks containing sterilized medium [33]. Cultures were then incubated under a surface light intensity of 45 μ mole photon m^{-2} s^{-1} at 30 °C and supplied with a mixture of 97% dry air and 3% CO$_2$ to accelerate growth. The pumped air was sterilized first by passing through bacterial air filters of 0.45-μ pore diameter. The cultures were grown until the beginning of the stationary phase corresponding to each species. For this study, *S. platensis* biomass was harvested on the 16th day, and *N. linckia* biomass was collected on the 22nd day of growth, at which the maximum content of phycobiliproteins was achieved. Cyanobacterial biomass was harvested by centrifugation (Centurion Scientific, Model: CR2000, UK) at 2000g for 20 min. Pellet cells were rinsed, washed three times with distilled water, and re-suspended in sterilized distilled water to remove traces of growth medium [34].

2.2 Extraction of Phycobiliprotein Pigment

Crude phycobiliproteins from *S. platensis* and *N. linckia* were extracted according to Bennet and Bogorad [35]. Whereby, the freezing and thawing techniques of cell suspension (50 ml) in distilled water were manifested for two times at 24-h

intervals to break the cells. The cells were then sonicated at a pulse of 60% for 15 min (Chromotech Ultra Sonic Processor). After sonication, the biomass was centrifuged at 2000g for 20 min to get the phycobiliprotein pigment. The procedures were repeated for 3 days for *S. platensis* and 7 days for *N. linckia*. Finally, the obtained volumes of the pigments were collected together and termed as "crude phycobiliprotein extract." The pigment components were estimated spectrophotometrically at 615 nm for phycocyanin (PC), at 652 nm for allophycocyanin (APC), and 526 nm for phycoerythrin (PE). The following equations were applied to calculate the concentration of each component:

PC = (E_{615} — 0.474 E_{652})/5.34

APC = (E_{652} — 0.208 E_{615})/5.09

PE = (E_{526} — 2.4 (PC) — 0.849 (APC))/9.62

where E is the absorbance value at each specific wavelength, and numbers are specific coefficients.

The crude phycobiliprotein extracts were then stored in a refrigerator at 4 °C in dark bottles until used for nanoparticle synthesis.

2.3 Biosynthesis of Silver Nanoparticles

For biosynthesis of AgNPs: of *S. platensis* and *N. linckia* crude phycobiliprotein extract (90 ml) was added to AgNO$_3$ (10 ml). The reduction of silver metal ions (Ag$^+$) to nanoparticles (Ag^0) took place at room temperature and pH 7. The visual appearance of a yellowish to brownish color in the solutions was an evident indication of AgNP formation [36].

2.3.1 Characterization of AgNPs

Ultraviolet-Visual Spectroscopy The developed color was monitored through aliquots sampling (0.2 ml) of the colloidal suspension diluted to 2 ml with deionized water and measured using ultraviolet-visual (UV-Vis) spectra of a double beam PC scanning spectrophotometer scanned at 200–800-nm range. The appearance of a plasmon resonance peak at 420 nm verifies the biosynthesis of AgNPs.

Fourier Transformer Infrared Analysis Fourier transformer infrared (FTIR) spectrophotometer (AKX, Genesis Series Nicolet, IS-10 F) was used to identify the functional groups in *S. platensis* and *N. linckia* crude phycobiliprotein extract which were responsible for the reduction of silver ions. Along with the range of 500 to 4000 cm^{-1}, the spectrum was chronicled.

Powder X-ray Diffraction Analysis The X-ray diffraction (XRD) dimensions were performed (Philips-X'Pert MPD X-ray diffractometer) to determine the size and the crystalline shape of the AgNPs. The dried NP powder was coated onto a glass substrate while scanned in the region of 2θ, from 4 to 90° at 0.5°/min with the time constant of 2 s. The mean particle diameter of AgNPs was designed from the XRD pattern according to the line width of the maximum intensity reflection peak using Scherrer's equation as:

$$D = (K\lambda)/(\beta\text{cor} \cos \theta)$$

"D" is the average crystal size, K is the Scherrer coefficient (0.89), λ is the X-ray wavelength ($\lambda = 1.5406$), °2θ is the Bragg's angle, βcor is the corrected full width at half maximum (FWHM) in radians, with βcor = (β2sample − β2ref) 1/2, and β sample and β ref. are the FWHM of the sample and reference peaks, respectively.

Transmission Electron Microscopy Transmission electron microscopy (TEM) analysis was employed to visualize the shape and confirm the size of the biosynthesized AgNPs. A drop of AgNPs on a carbon-coated TEM grid was allowed to dry at room temperature before analysis. TEM was carried out using JEOL-JEM 2100 Electron microscope functioning at 80 KV and a magnification of × 20,000 and a resolution up to 100 nm for micrographs.

Zeta Potential Analysis Zeta potential of the biosynthesized AgNP aqueous suspensions was determined by placing 2 ml of the samples in a four-sided clear plastic cuvette in a Malvern zeta sizer instrument (Malvern instrumentation Co.) at 25 °C. The measurement was performed directly in the clear disposable zeta cell.

2.3.2 Applications of Biosynthesized AgNPs

Antimicrobial Activity of AgNPs Five pre-identified bacterial pathogenic strains were obtained from Bacteriology Laboratory, Faculty of Science, Tanta University. Microbial suspensions were prepared in a sterile saline solution (0.9% w/v NaCl) at a turbidity of 10^6 to 10^8 CFU/ml. The Gram-negative bacterial strains *Escherichia coli*, *Klebsiella pneumoniae*, and *Proteus vulgaris* were cultivated in MacConkey solid medium, and Gram-positive bacterial strains *Diplococci* sp. and *Staphylococcus aureus* were grown onto nutrient agar medium [37]. One fungal strain, *Candida albicans*, was cultivated on Sabouraud Dextrose agar medium. The antimicrobial activities of the biosynthesized AgNPs were evaluated using the disk diffusion method [38]. Sterilized paper disks loaded with 15, 30, and 60 µg/disk of AgNPs were placed in the Petri dishes pre-inoculated with 100 µl of each microorganism suspension and then incubated at 37 °C. Positive control of standard antibiotics was tested and also negative controls of AgNO$_3$ solution and

cyanobacterial phycobiliprotein crude extract. After the incubation period, the inhibition zone diameters were measured and compared to the standard reference table of antibiotics [38]. The positive antibacterial controls were ciprofloxacin (CIP), doxycycline (DO), and ampicillin-sulbactam (SAM), while the antifungal positive controls were fluconazole (FLU), itraconazole (ITC), and metronidazole (MT).

2.3.3 Antioxidant Activity of AgNPs

DPPH Radical Scavenging Activity The capacity of AgNPs to reduce 2,2-diphenyl- picrylhydrazyl (DPPH) stable free radical was assessed as described by Blois [39]. Three hundred microliters of AgNPs at various concentrations was mixed with 2.7 ml of DPPH reagent solution and allowed to stand for 30 min in the dark at room temperature. The absorbance of the samples was measured at 517 nm, and DPPH only was also detected as a negative control. The antioxidant capacities of the samples were compared with ascorbic acid as a standard. The IC_{50} value of DPPH and ascorbic acid was also calculated. The DPPH scavenging activity was calculated as a percentage according to the following formula:

Inhibition of the DPPH activity $(\%)$

$$= (A_c - A_s)/(A_c) \times 100$$

where A_c is the absorbance of the control and A_s is the absorbance of the sample.

Total Antioxidant Capacity Assay The total antioxidant activity of AgNPs was evaluated by the phosphomolybdenum method [40]. Different concentrations of AgNPs were prepared by dissolving a known weight of AgNPs in 10 ml of 1 mM dimethyl sulfoxide. Three hundred microliters of each concentration was added to 3 ml of phosphomolybdate reagent solution (0.6 M sulfuric acid, 28 mM sodium phosphate, and 4 mM ammonium molybdate). The reaction was protected from light, and then the vials were incubated for 90 min in a water bath at 95 °C. The absorbance was measured at 695 nm against a blank after cooling the mixture at room temperature. Ascorbic acid was used as a reference. Results were expressed as mg ascorbic acid/g dry wt of the NPs (mg AAE/g DW).

The Ferric Reducing Antioxidant Power Assay The chelation activity of ferrous ions by AgNPs was estimated as described by Do et al. [41]. First, 1 ml each of different AgNP concentrations was added to 2.5 ml of sodium phosphate buffer (0.2 mM, pH = 6.6) and 2.5 ml of potassium ferrocyanate (1%) then the mixture was incubated for 20 min in a water bath at 50 °C. After that, 2.5 ml of tricholoroacetic acid (10%) was added before centrifugation of the mixture solution at 500 g for 10 min. Then, 5 ml of the supernatant was mixed

with 5 ml dist. H_2O and 1 ml of ferric chloride solution (0.1%). The absorbance of the mixture was measured at 700 nm. Higher absorbance values indicate increased reducing power. The results were reported as ascorbic acid equivalents (AAE) per gram dried sample (mg AAE/g DW).

2.3.4 Antiviral Activity of AgNPs

Mammalian Cell Culture Conditions Mammalian cells, hepatocellular carcinoma, and HepG2 were obtained from VACSERA, Egypt. And then were cultured in Dulbecco's modified Eagle's medium (DMEM) supplemented with 2 mM of L-glutamine, 10% of fetal bovine serum (FBS), and 1% penicillin-streptomycin solution in 50-ml cell culture flasks, incubated at 35 °C in a humidified atmosphere of 5% CO_2 and 95% air for 24 h. For experimental purposes, cells were cultured in 6-, 12-, or 96-well plates.

2.3.5 Cytotoxicity Test

Through this test, the maximum non-cytotoxic concentration of the test sample was determined. This concentration was used for all tests without having any toxic effect on the cells [42]. Staining vital cells with neutral red has been known for a long time. Only vital cells can incorporate neutral red into the liposome, so, the amount of absorbed stain is proportional to the number of vital cells [43]. Peripheral Blood Mononuclear Cells (PBMC) were plated into 96-well plates at a cell count of 5×10^4 cell ml^{-1}. After 24 h of incubation, the cells were semi-confluent, and serial dilution of the AgNPs in culture medium was added. The treated cells were then incubated for 3 days at 37 °C and 5% CO_2 supply, during which they were exposed to a serial dilution of the AgNPs. After that, 100 μl of neutral red was added to every well, and the plates were incubated for 3 h. Thereafter, cells were fixed with 100 μl fixative solution (0.5 formaldehyde and 1% $CaCl_2$) for 1 min. Then, each well was supplemented with 100 μl solution of ethanol with 1% acetic acid while shaking for 5 min. Finally, the adsorption of plates was measured at 450 nm. Plotting concentrations against the percentage of cell survival gave a cytotoxicity curve, from which the maximum non-cytotoxic concentration was determined and used afterward in the following experiments. From the same curve, the IC_{50} toxic concentration value was also calculated [43].

Determination of Virus Concentration Hepatitis C virus (HCV) concentration was firstly determined by real-time polymerase chain reaction (RT-PCR).

2.3.6 Antiviral Assay

Non-toxic concentrations of the AgNPs in 50 ml of DMEM-supplemented medium were added simultaneously with the

virus (infected serum, 8.3×10^6 copies/ml, genotype 4a) to the host cells (HepG2, 10^5 cells/ml). After 90-min incubation period, the infected cells were washed three times with 1 ml of phosphate-buffered saline (PBS) and further cultured for 3 days at 37 °C and 5% CO_2, and then total RNA extraction had done.

Extraction of RNA from HepG2 Cells The positive and/or negative HCV RNA strand was separated from HepG2 cells, which was reported by Lohr et al. [44]. Briefly, cells were precipitated and washed in the same buffer to remove adherent viral articles, then lysed in 4 mol/l guanidinium isothiocyanate (containing 25 mmol/l sodium citrate, 8 µl β-mercaptoethanol, 5% sacrosyl, and 100 µl sodium acetate). Five hundred microliters of phenol (pH = 4) and 200 µl of chloroform were added then vortexed. The lysed cells were centrifuged at 12000 rpm for 20 min at 4 °C. The upper aqueous layer was transferred to new falcons and mixed with the same volume of isopropanol and incubated overnight at 20 °C. RNA was precipitated by centrifugation at 12000 rpm for 20 min at 4 °C. The precipitate was washed with 70% ethanol, and the previous centrifugation procedures were repeated twice.

PCR of Genomic and Antigenomic RNA Strands of HCV Reverse transcription polymerase chain reaction (RT-PCR) was done following the method of Lohr et al. [44] with some modification. Reverse transcription was performed in 25-µl reaction mixture which contains 20 U of AMV (alfalfa mosaic virus) reverse transcriptase, 2 mmol/l from each of dNTP (Deoxy Nucleotide Triphosphate; Promega, Madison, WI, USA) with 50 pmol of reverse primer 1CH used as plus strand and 50 pmol of forwarding primer 2CH used as a minus strand. This reaction had been incubated for 60 min at 42 °C then denatured for 10 min at 98 °C. Two rounds of PCR with two pairs of nested primers were used for amplification of highly conserved 5′–UTR sequences. A reaction mixture of 25 µl that contains 50 pmol from each of 2CH forward primer and P2 reverse primer was carried out for first-round amplification. 0.2 mmol/l of dNTP, 10 µl from RT reaction mixture (template and 2 U of Taq DNA polymerase in 1X buffer) were added to the reaction mixture. Then a protocol of 1 min at each of 94 °C, 55 °C, and 72 °C for 30 cycles, which was described as a thermal cycling protocol, was applied. Then the second round amplification has been carried out as the first one, excluding the use of nested reverse primer D2 and the forward primer F2 at 50 pmol. A fragment of 174 bp had been recognized in positive samples. The primer sequences used in the reaction were:

1CH: 5′-GGTGCACGGTCTACGAGACCTC-3′,
2CH: 5′-AACTACTGTCTTCACGCAGAA-3′,
P2: 5′-TGCTCATGGTGCACGGTCTA-3′,
D2: 5′-ACTCGGCTAGCAGTCTCGCG-3′ and

F2: 5′-GTGCAGCCTCCAGGACCC-3′.

Strand-Specific RT-PCR The final PCR product was checked by the RT-PCR, which constructed on SYBR Green 1 dye and light Cycler fluorimeter method that use standard serum samples infected by HCV. During PCR of the 5′ HCV non-coding (NC) region, the SYBR Green 1 dye binding to double-stranded DNA for the synthesis of amplicon that continuously monitored and specifically verified by temperatures of amplicon melting. A serial of a modified synthetic HCV 5′ NC RNA of 10-fold dilutions was created with an external standard curve. After the RT step, the first-round PCR, which uses 2CH and P2 primers in 25-µl reaction mixture that contains 3.5 µl cDNA, 50 pmol of 2CH forward primer, 50 pmol of P2 reverse primer, and 12.5 µl of SYBR Green master mix, was done, then the previous thermal cycling protocol of 30 cycles of 1 min at 94 °C, 55 °C and 72 °C with final extension made for 5 min at 72 °C [45].

Statistical Analysis One way analysis of variance (ANOVA) was performed for the results of the antimicrobial test. The difference between means pigments and antioxidant results (total antioxidant capacity (TAC) and FRAB) in both cyanobacteria series was tested by using an unpaired t - test. All results were expressed as a mean of three replicates ± standard deviation (SD) and statistically evaluated using SPSS 16.0 software SPSS (2006) [46].

3 Results

3.1 Estimation of Pigment Concentration in the Crude Phycobiliprotein Extract

The PC, APC, and PE pigment components in the crude phycobiliprotein extract are shown in Table 1 for *S. platensis* and *N. linckia*. *N. linckia* exhibited a highly significant total pigments composition (0.307 mg/ml), of which PC value was the maximum (0.158 mg/ml).

3.2 Visual Biosynthesis and Ultraviolet-Visual Spectroscopy of AgNPs

Reduction of the silver ion to AgNPs by crude phycobiliprotein extracts of *S. platensis* and *N. linckia* was followed by a visual change of solution color to reddish-brown, as shown in Fig. 1. The change in color indicated the formation of AgNP solution through the biotransformation of the ionic silver (Fig. 1). For the characterization of the formed AgNPs, the UV-Vis absorption peak was monitored at a time interval of 2, 6, 12, and 24 h for *S. platensis* AgNPs (Fig. 2a) while at 24, 48, 72, and 96 h for *N. linckia* ones (Fig. 2b). The

Table 1 Concentration of pigments (mg/ml) in the crude phycobiliprotein extract of *S. platensis* and *N. linckia*

Species	PC	APC	PE	Total phycobiliproteins
S. platensis	0.135±0.002	0.072±0.00	0.048±0.001	0.255±0.001
N. linckia	0.158±0.001	0.093±0.002	0.056±0.002	0.307±0.001
t value*	12.57***	17.19***	4.13**	31.84***

All values are mean of three replicates ± SD. *t* values* show significant differences at $p** \leq 0.01$ and $p*** \leq 0.001$.

surface plasmon resonance bands at 420 nm indicated the production of AgNPs of *S. platensis* and *N. linckia* phycobiliprotein crude extracts. Although the peak intensity of both species was nearly the same, the formation of AgNPs by *S. platensis* phycobiliproteins was markedly faster. By increasing the period of incubation time, the peak at 420 nm got sharper and narrower because of the completed construction of AgNPs. These results also indicated that AgNPs were dispersed in the aqueous solution with no evidence for aggregation, and its formation was dependent on the time and the algal extract source.

3.3 Fourier Transformer Infrared

The functional groups of the biomolecules in *S. platensis* and *N. linckia* phycobiliprotein extracts were identified by FTIR. The FT-IR spectrum of *S. platensis* AgNPs (Fig. 3a) showed various absorption peaks (cm^{-1}) at 3796 and 3430 which indicates the presence of OH strong stretching band of alcohols or phenols, respectively. The peak at 2925 represents N–H group (amino acids), and at 2426 and 2360 represent C=O of the carboxylic anion. The peak at 1634 indicates the presence of broad stretching aliphatic bond of carboxylate group C=O; at 1383 represents a strong sharp band of C–H or CH_3 methyl group; at 1153 is a broadband carboxyl of carboxylic acid C–O–C and at 875 is a broad weak band of C–O–S sulfate group. Similarly, the FT-IR spectrum of *N. linckia* AgNPs (Fig. 3b) showed strong absorption peaks at 3872, 3384, and 3210 cm^{-1} due to O–H stretching vibration presence of alcohols or phenols, while the peaks at 2964 and 2924 can be assigned to stretching broadband of N–H group (amino

acids). The peaks at 2426, 2363, and 1641 cm^{-1} represented the protein amide, mainly C=O stretching broad, which may be due to the N–H bending vibration of the carbonyl β unsaturated ketone amide and secondary amines (protein, lipid). The peak at 1383 represents a strong, sharp band of C–H or CH_3 methyl group, and the bands at 1044 and 877 were allocated to the stretching vibrations of primary and secondary amines, respectively.

3.4 Powder X-ray Diffraction

The XRD analysis showed intense peaks corresponding to 111, 200, 220, and 311 Bragg reflections of the biosynthesized AgNPs (Fig. 4a and b), which indicated a crystalline nature of the formed nanoparticles. The average crystal size was calculated from the FWHMs of the diffraction peaks using Scherrer's equation. The FWHMs of all detected peaks of *S. platensis* AgNPs were at 38.6° (111), 44.8° (200), 64.8° (220), and 77.9° (311), while the FWHMs of all peaks of *N. linckia* AgNPs were at 38.55° (111), 44.6° (200), 64.5° (220), and 77.3° (311) in °2θ which were used for size evaluation. The average estimated size was 21.05 nm and was 20.84 nm for *S. platensis* and *N. linckia* AgNPs, respectively. A more broadening of the Bragg peaks indicated more reduction in the grain size.

3.5 Transmission Electron Microscopy

TEM is a commonly used technique for characterizing the size and shape of the biosynthesized nanoparticles. All the particles were spherical. The particle size distribution of
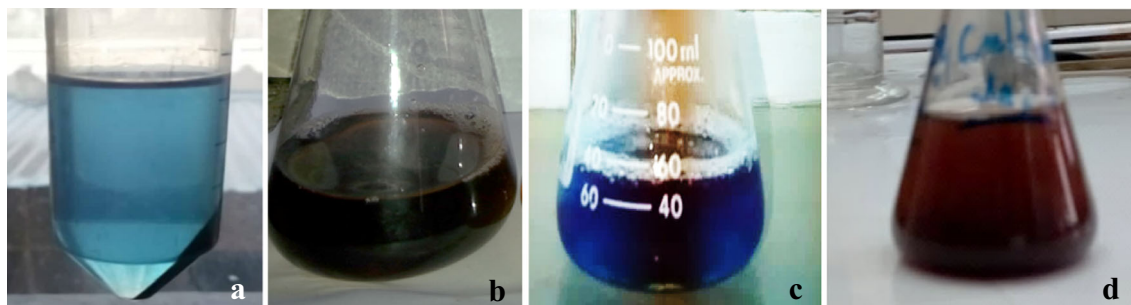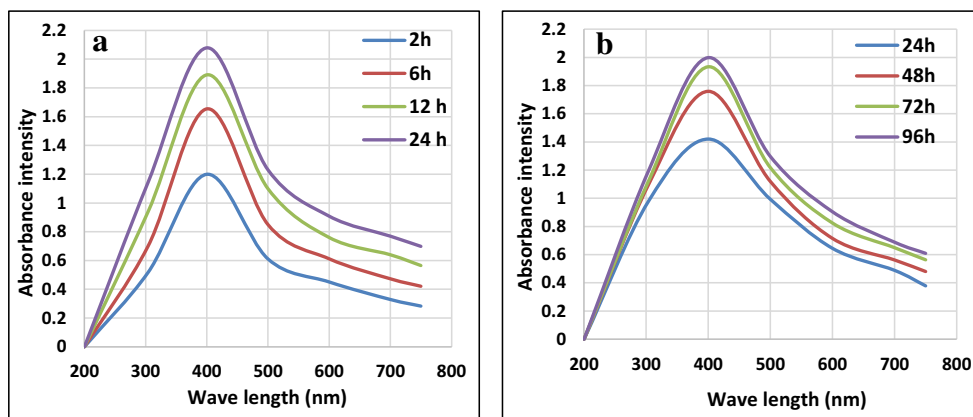

Fig. 1 *S. platensis* crude phycobiliprotein extract (**a**) and its biosynthesized AgNPs (**b**); *N. linckia* crude phycobiliprotein extract (**c**) and its biosynthesized AgNPs (**d**)

Fig. 2 UV-Vis spectra of AgNPs synthesized by crude phycobiliprotien extract of *S. platensis* (**a**) and *N. linckia* (**b**)


S. platensis AgNPs was ranged from 15.1 to 27.4 nm with a mean particle size of 21.211 nm. For the AgNPs formed by *N. linckia*, the particle size distribution was in the range of 16.3 to 25.8 nm with a mean particle size of 21.052 nm (Fig. 5a and b).

3.6 Zeta Potential Analysis of AgNPs

Zeta potential analysis verified the stability of the biosynthesized AgNPs. A net charge of − 15.902 ± 4.87 mV and − 16.811 ± 6.99 mV with a conductivity of

Fig. 3 FT-IR spectra of AgNPs synthesized by phycobiliprotein crude extract of *S. platensis* (**a**) and *N. linckia* (**b**)
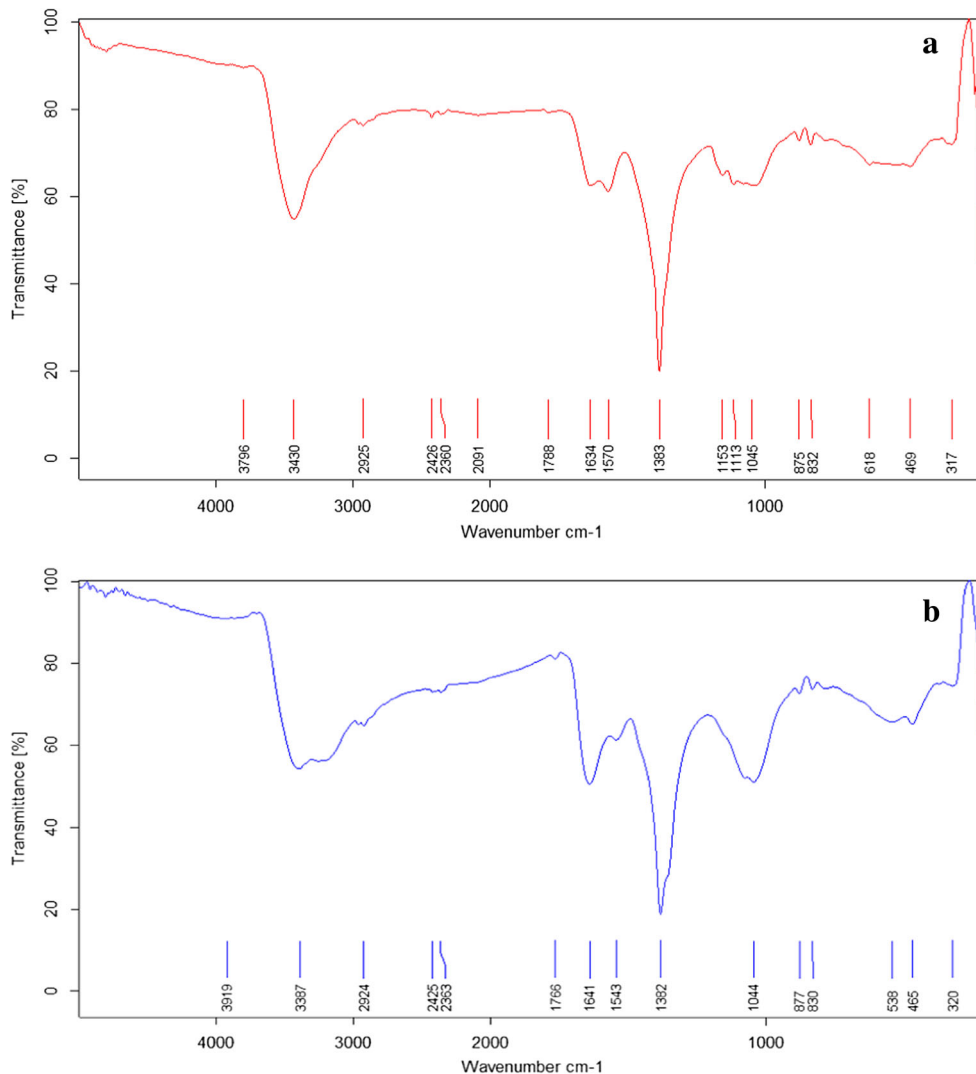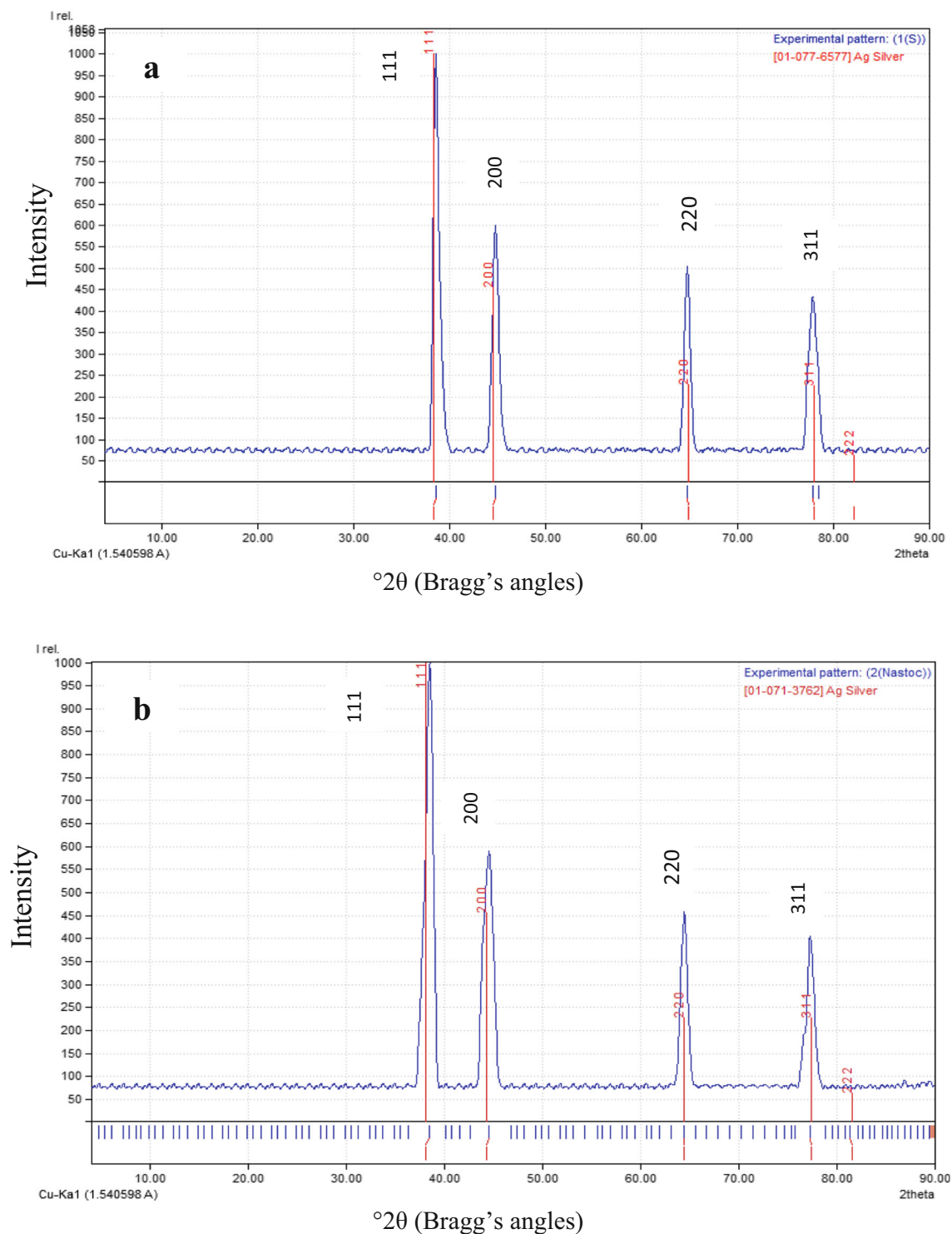
Fig. 4 XRD analysis of AgNPs synthesized by crude phycobiliprotein extract of *S. platensis* (**a**) and *N. linckia* (**b**)

0.225 and 0.23 mS/cm were detected for *S. platensis* and *N. linckia* AgNPs, respectively (Fig. 6a and b). The zeta potential of nanoparticles that is greater than + 30 mV or less than − 30 mV has sufficient electrostatic repulsion to remain stable in solution [25].

3.6.1 Antimicrobial Activity of AgNP

The bactericidal activity of *S. platensis* and *N. linckia* AgNPs was performed against five pathogenic bacterial species: two were G+ve bacteria of *Diplococci* sp. and

Fig. 5 TEM image of AgNPs by phycobiliprotein crude extracts of *S. platensis* (**a**) and *N. linckia* (**b**)
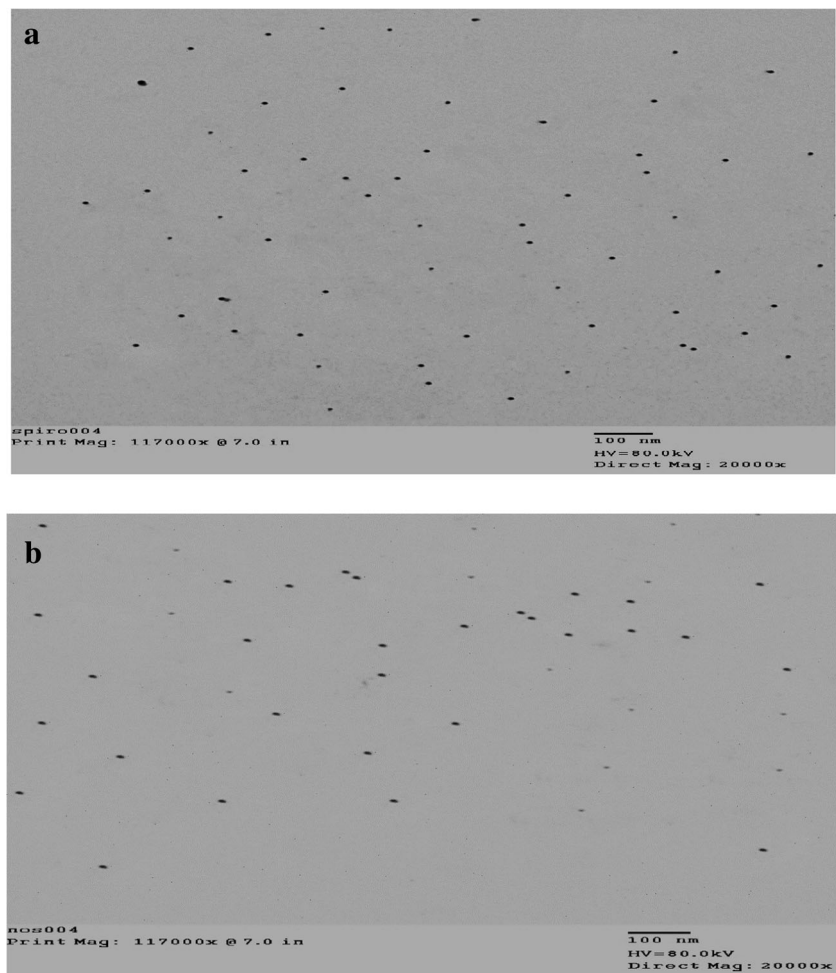
Staphylococcus aureus and three were G–ve bacteria of *E. coli*, *K. pneumoniae*, and *P. vulgaris* in addition to *Candida albicans* fungal strain. By increasing the concentration of AgNPs, the diameter of the inhibition zones also increased (Table 2). At the lowest AgNP concentration of 15 μg/ml, the diameter of different inhibition zones was insignificant compared to those recorded for the negative controls, especially with *S. platensis* AgNPs. At the highest concentration of 60 μg/ml, an elevated inhibitory effect was observed for AgNPs biosynthesized by *S. platensis* crude phycobiliprotein extract against *P. vulgaris* (15.5 mm), *Diplococci* sp. (14 mm), and *S. aureus* (12.1 mm). At the same concentration of *N. linckia* AgNPs, a higher significant inhibition zones were recorded against *Diplococci* sp. (20 mm), *S .aureus* (17.8 mm), *P. vulgaris* (15 mm), and *K. pneumonaie* (13.75 mm) compared to the antibacterial positive controls. A moderate antifungal activity against *C. albicans* was recorded for AgNPs of *N. linckia* (10.5 mm) and *S. platensis* (9.8 mm) compared to the significant antifungal controls, especially for MT and FLU. As a negative control, $AgNO_3$ solution and crude phycobiliprotein extracts of *S. platensis* and *N. linckia*

treatments showed insignificant, weak inhibitory effects against G−ve rather than G+ve bacterial as well as the fungal strain tested pathogens (Table 2).

3.6.2 Antioxidant Activity of AgNPs

DPPH Radical Scavenging Activity The IC_{50} value of DPPH scavenging activity was considerably higher (133.8 μg/ml) for *S. platensis* phycobiliprotein AgNPs than that of AgNPs synthesized by *N. linckia* crude phycobiliprotein extract, which records 77.3 μg/ml. In the present study, increased concentrations of AgNPs showed comparatively higher DPPH antioxidant activity (Table 3) compared to ascorbic acid (AA) as standard antioxidant. The IC_{50} value of ascorbic acid was 67 μg/ml.

Total Antioxidant Capacity By increasing AgNP concentration, the total antioxidant capacity increased too (Fig. 7a). The biosynthesized AgNPs showed significant phosphomolybdenum reduction activity (at $p \leq 0.001$), recording 44.57 and 45.13 mg AAE/g DW for *S. platensis* and *N. linckia* AgNP crude phycobiliprotien extracts, respectively at 300 μg/ml.
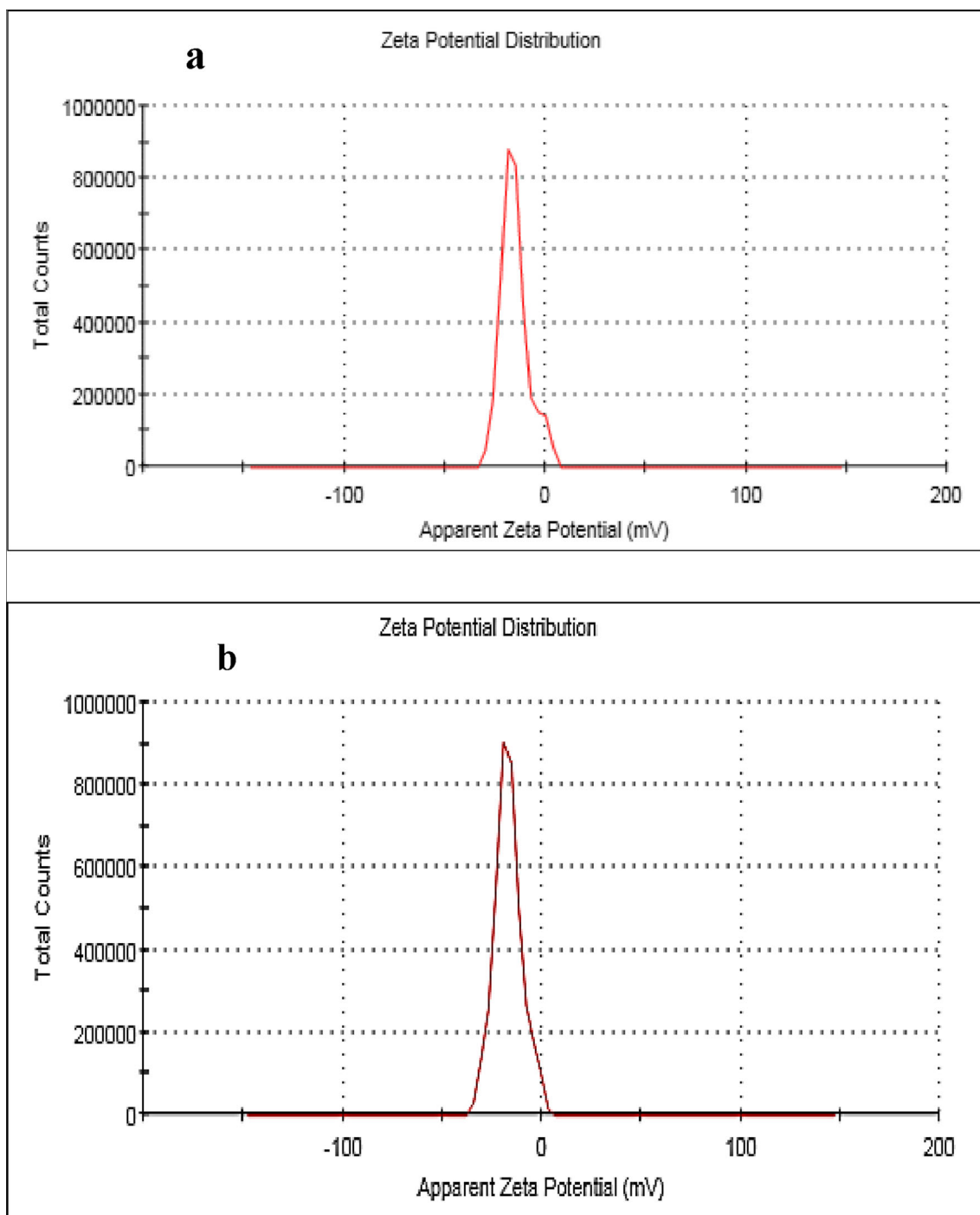
Fig. 6 Zeta potential analysis of AgNPs synthesized by crude phycobiliprotein extracts of *S. platensis* (**a**) and *N. linckia* (**b**)

Ferric Reducing Antioxidant Power Similar behavior was observed using FRAP assay as that observed for TAC assay where the antioxidant activity for both *S. platensis* and *N. linckia* phycobiliprotein AgNPs exhibited significant difference values of 34.75 and 35.13 mg AAE/gDW, respectively at the concentration of 300 μg/ml (Fig. 7b).

3.6.3 Antiviral Activity of AgNPs

Cytotoxicity of the Biosynthesized AgNPs on HepG2 Cell Line The cytotoxicity of *N. linckia* and *S. platensis* phycobiliprotein extract AgNPs on human liver carcinoma (HepG2) cell line was assessed using the neutral red assay. At lower concentration of 16 μg/ml, the cell viability recorded

Table 2 Diameters of inhibition zones (mm) of AgNPs synthesized by crude phycobiliprotein extracts of *S. platensis* and *N. linckia* compared to antibiotics, antifungal, and negative controls

Treatments	Potency (μg/ml)	Zones of inhibition (mm)					
		K. pneumoniae	*E. coli*	*P. vulgaris*	*Diplococci* sp.	*S. aureus*	*C. albicans*
S. platensis AgNPs	60	9.10±0.0[c]	4.00±0.0[d]	15.5±0.5[a]	14.00±0.3[b]	12.10±0.1[b]	9.80±0.1[c]
	30	6.05±0.0[d]	2.43±0.0[e]	9.01±0.1[c]	9.72±0.2[c]	9.50±0.1[c]	4.50±0.1[d]
	15	2.95±0.1[f]	1.37±0.1[f]	4.45±0.2[d]	5.82±0.2[d]	6.11±0.0[d]	2.10±0.1[e]
N. linckia AgNPs	60	13.75±0.3[a]	9.11±0.0[c]	15.03±0.3[a]	20.12±0.3[a]	17.8±0.1[a]	10.51±0.2[c]
	30	9.45±0.1[c]	4.60±0.2[d]	8.71±0.2[c]	13.83±0.2[b]	11.00±0.1[b]	6.35±0.1[d]
	15	4.51±0.0[d]	2.30±0.0[e]	3.90±0.1[d]	7.31±0.2[d]	7.21±0.2[d]	3.82±0.0[e]
Antibiotics	CIP	12.83±0.3[b]	R	11.81±0.3[b]	10.61±0.0[c]	9.60±0.0[c]	-
	DO	R	13.01±0.3[a]	12.00±0.3[b]	6.32±0.1[d]	R	-
	SAM	14.22±0.0[a]	10.22±0.2[b]	R	8.43±0.0[c]	16.53±0.3[a]	-
Antifungals	FLC	-	-	-	-	-	13.21±0.0[b]
	ITC	-	-	-	-	-	9.11±0.0[c]
	MT	-	-	-	-	-	16.73±0.0[a]
Negative controls	AgNO₃	2.12±0.0[f]	2.44±0.1[e]	3.90±0.1[d]	4.30±0.1[e]	5.15±0.2[d]	2.23±0.1[e]
	S. platensis phycobiliproteins	2.91±0.1[f]	1.53±0.0[f]	R	2.92±0.2[f]	3.23±0.0[e]	1.81±0.0[f]
	N. linckia phycobiliproteins	3.33±0.0[e]	2.31±0.0[e]	R	4.42±0.1[e]	2.33±0.0[f]	1.62±0.0[f]

Values are mean of three replicates ± SD. Values with different superscript letter in the same column showed significant differences at $p \leq 0.01$. The value equal 0.00 mm means no inhibition zone was recorded, i.e., the pathogen was resistant (R)

90% ± 0.2 and 93% ± 0.2; while at 1000 μg/ml, the cell proliferation decreased to 48.1% ± 0.5 and 53.3% ± 0.4 for *S. platensis* and *N. linckia* AgNPs, respectively. As the AgNP concentration increased, the cell viability decreased in a direct dose-response relationship (Fig. 8). The concentration necessary to produce 50% of tumor cell death (IC_{50}) was 992 μg/ml for *S. platensis* AgNPs, while the same concentration for *N. linckia* AgNPs was not detected indicating that *N. linckia* AgNPs were safer in the tested concentration range. Thus, the concentration of 16 μg/ml AgNPs was chosen for the rest of the experiment as the safe dose (Fig. 8).

Antiviral Activity Assay Using RT-PCR Technique Results indicated that the antiviral activity of Ribavirin, as a standard antiHCV drug, recorded 66.673%. AgNP phycobiliprotein crude extract of *N. linckia* recorded 64.976% which compared effectively to Ribavirin (at $p \leq 0.05$), while *S. platensis* AgNPs showed a lower potent activity of 48.334% (Table 4).

4 Discussion

In cyanobacteria, phycobiliproteins are responsible for harvesting the light and deliver it to chlorophyll. Phycobiliprotein pigments (PBPs) can be classified into three types of phycocyanin (PC), phycoerythrin (PE), and allophycocyanin (APC), according to their maximum absorbance [27]. Many researchers reported the synthesis of AgNPs by cyanobacterial filtrate and biomass [47, 48]; only a few reports are available regarding the phycobiliproteins of cyanobacteria for the synthesis of NPs [15]. The synthesis of AgNPs was originally determined by the visual change in the color of silver nitrate solution from colorless to reddish-brown. Our result clearly showed that phycobiliprotein crude extract from *N. linckia* and *S. platensis* efficiently reacted with AgNO₃ to form AgNPs by a reduction process in a range of 24 to 96 h of incubation time. By using the UV-Vis spectroscopy, the surface plasmon band of the biosynthesized AgNPs was at

Table 3 DPPH radical scavenging activity of AgNPs synthesized by crude phycobiliprotein extracts of *S. platensis* and *N. linckia*

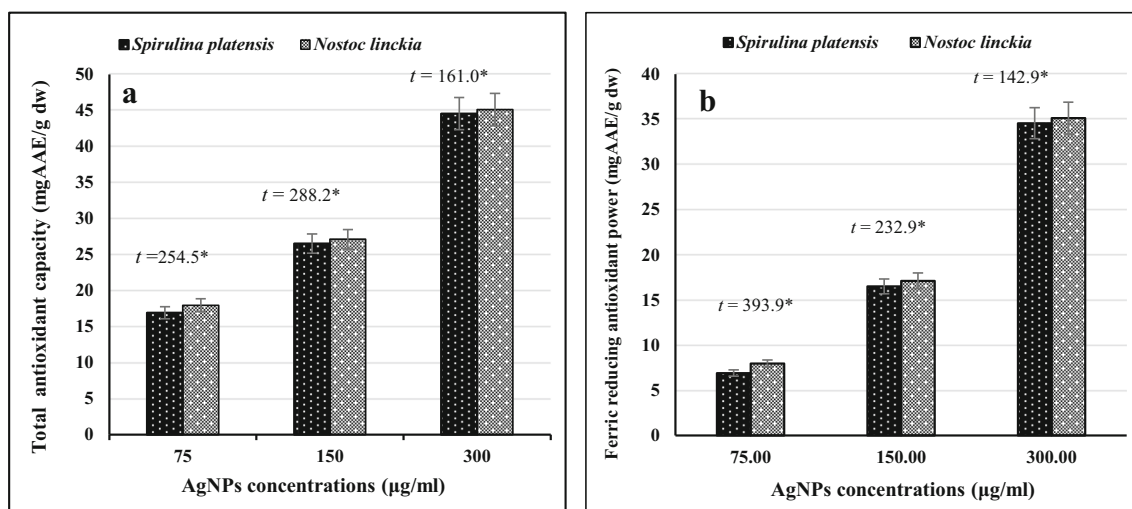| Concentrations of AgNPs (μg/ml)	*S. platensis* AgNP scavenging activity (%)	*N. linckia* AgNP scavenging activity (%)
300	69.0	77.0
150	57.8	68.5
75	46.0	55.3
38	36.5	43.0
19	29.0	34.1

Fig. 7 Antioxidant activity of AgNPs synthesized by crude phycobiliprotein extracts of *S. platensis* and *N. linckia*: Total antioxidant capacity (**a**), ferric reducing antioxidant power (**b**). All mean values are of significant difference at $p \leq 0.001$

420 nm throughout the reaction period, indicating that NPs were stable and well dispersed in the solution. Electrostatic interaction between the silver ions and the negatively charged carboxylate groups, which are present in phycobiliproteins, is thought to be the first step that involves the trapping of metal ions on the surface of algal cells [49]. The spectra of AgNPs were also dependent on the size, shape, and incubation time of the particles. The results showed that reduction of Ag^+ ions into Ag^0 started within 2 h after the addition of $AgNO_3$ solution to *S. platensis* phycobiliprotein extract and completed after 24 h of incubation, while started within 24 h for *N. linckia* phycobiliprotein extract and completed after 96 h (Fig. 1a and b). This indicates the rapid synthesis and stability of the biosynthesized AgNPs. The obtained results were compatible with those reported in [15, 50].

FTIR indicated that AgNPs biosynthesized by *S. platensis* and *N. linckia* phycobiliproteins have nearly the same peaks, which represent similar functional groups, but most important changes in stretching frequencies were observed after the synthesis of AgNPs. The involvement of several functional groups such as hydroxyl, carboxyl, and carbonyl groups of amino acids

and proteins were logged that might be responsible for the reduction of silver ions and also for capping of the bio-reduced AgNPs [51] as well as stabilization of these NPs for long duration by avoiding their aggregation and growth in the solution. The presence of some aromatic amino acids like tryptophan, phenylalanine, and tyrosine in the composition of phycobiliproteins and which induces the formation of AgNPs makes phycobiliproteins play a great important role in the synthesis and stabilization of metal NPs [52]. In agreement with our results, Mubarak-Ali et al. [48] reported the existence of cyanobacterial protein covering around Cd–S nanoparticles from cyanobacteria *Oscillatoria welli*, which was accounted for the NP biosynthesis. These protein molecules boosted the formation of AgNPs with a particularly small size and narrow particle distribution. On the other side, the presence of sulfonic and hydroxyl groups is useful for the biosynthesis of AgNPs with rather larger particle size [48]. In addition, besides providing stability and capping, the presence of phycobiliprotein biomolecules may offer anchoring ability to the developed NPs on bacterial cell membranes, enabling them to achieve antibacterial activity as reported by El-Naggar et al. [15].

Fig. 8 Cytotoxicity of AgNPs biosynthesized by *S. platensis* and *N. linckia* phycobiliprotein crude extract on human liver cancerous (HepG2) cell line
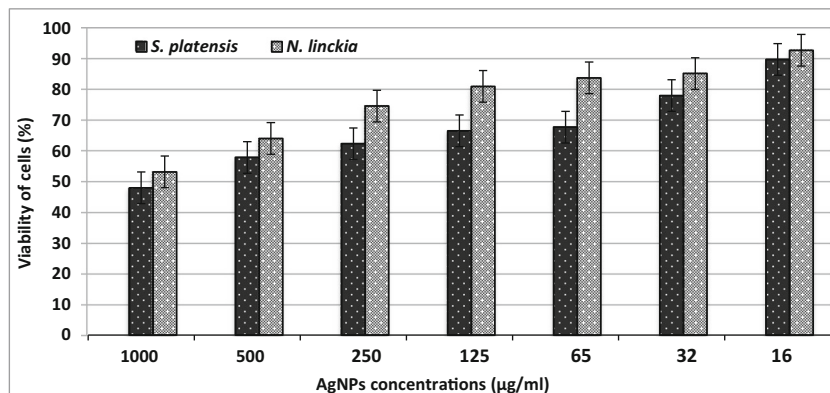
Table 4 Antiviral assay of AgNPs synthesized by crude phycobiliprotein extracts of *S. platensis* and *N. linckia* on hepatitis C virus

Virus treatment	% inhibition of HCV
Ribavirin (standard drug for HCV)	66.673 ± 1.5
AgNPs synthesized by *N. linckia* phycobiliproteins	64.976 ± 1.6
AgNPs synthesized by *S. platensis* phycobiliproteins	48.334 ± 1.4

In this study, the average size of the developed AgNPs was 21.05 and 20.84 nm for *S. platensis* and *N. linckia* respectively, as estimated from the FWHM of the four peak planes of silver ions. The crystalline nature of the nanoparticles by having a face-centered cubic (FCC) structure was confirmed by XRD analysis. AgNPs were found to be spherical in shape and well distributed in the solution. These results were in conformity with those reported by [53, 54]. TEM technique was also applied in this study to assess the particle size measure and the morphological shape of the biosynthesized AgNPs. From TEM images, AgNPs were spherical and well distributed with an average size below 25 nm for AgNPs of both *S. platensis* and *N. linckia* extracts. These results were in agreement with those reported by Shivaji et al. [53], who assessed that AgNPs are predominantly spherical.

The zeta potential is a physical property that is exhibited by any particle in suspension and predicting the long-term stability of these particles. The surface potential of the particles is reflected by its zeta potential and is influenced by the interface changes with the dispersing medium, due to the dissociation of the functional groups on the particle surface or to the adsorption of ionic species present in the aqueous dispersion medium [55]. A relatively high value of the zeta potential is important for good physical and chemical stability of the colloidal suspension because large repulsive forces tend to prevent aggregation due to incidental collisions of adjacent nanoparticles. Nanoparticles with zeta potential signal greater than + 30 mV or less than − 30 mV are considered strongly cationic and strongly anionic, respectively [15, 25]. In this connection, the biosynthesized AgNPs by *S. platensis* and *N. linckia* phycobiliproteins are considered strongly anionic which is important in the biological application, according to Aiad et al. [56].

The antimicrobial activity of biologically fabricated AgNPs has been reported by many researchers [54, 57]. As the extensive use of several synthetic antimicrobial agents has led to multidrug resistance in a number of bacterial strains, the results of the present study seems to be remarkable because the synthesized AgNPs showed strong antibacterial activity against five multidrug-resistant bacteria, *E. coli*, *K. pneumoniae*, *P. vulgaris*, *S. aureus*, and *Diplococci* sp., especially for *N. linckia* at the highest tested concentration of 60 µg/disk. Generally, as the concentrations of AgNPs increased, the diameter of the inhibition zone was increased too. The recorded variances in sensitivity among the tested

bacteria against AgNPs might be due to their differences in the building of their bacterial cell wall. Gram-positive bacteria have a thick peptidoglycan layer (20–30 nm) between the cytoplasmic membrane and the outer—non-lipid—membrane, while Gram-negative bacteria possess a thin peptidoglycan layer of about 3 nm in thickness and have an outer lipid membrane. This may be the cause of the high antibacterial activity of AgNPs on *S. aureus* and *Diplococci* sp. G+ve strains. For such strains, this effect was significantly pronounced even at the lowest tested concentration of 15 µg/disk compared to the negative controls (especially for *N. linckia* AgNPs, implying the antimicrobial efficacy of phycobiliproteins as nanoform). The small size of the volume area of AgNPs and its crystalline structure are responsible for their antimicrobial potentials and can change the membrane permeability by causing perforations/pits in the bacterial cell wall, and thus releasing vital membrane proteins and lipopolysaccharide molecules [47]. Other scientists suggested that the cell damage may be caused by the interaction of the released silver ions, Ag^+, with phosphorus and sulfur-containing compounds such as DNA and proteins, which in sequence lead to the detention of cell metabolic activities [14, 15]. Another potential pathway of the antimicrobial action is that, upon contact of AgNPs with bacteria, Ag^+ ion release, disturb the reduction of intracellular O_2, and interact with respiratory chain proteins on cell membranes, thus trigger free radicals and reactive oxygen species (ROS). This induced cellular oxidative stress could modulate the intracellular signaling routes of microbes' cells in the direction of apoptosis [58]. All these findings supported the potential antibacterial activity of AgNPs synthesized by phycobiliprotein extract from *S. platensis* and *N. linckia*.

In the present study, the DPPH scavenging method confirmed that AgNPs have antioxidant activities due to the presence of functional groups on their surface [59]. DPPH is a stable nitrogen-centered radical; the higher the antioxidant activity of the sample is achieved by its higher DPPH radical scavenging activity. This nominated AgNPs of *N. linckia* phycobiliproteins to be a more active antioxidant than *S. platensis* ones. Nevertheless, both NPs presented potent significant antioxidant capacity by using phosphomolybdenum and FRAP assays. It should be noted that in the ferrozine and phosphomolybdenum assays, the electron transfer occurs at different redox potentials, and in each case, the reducing activity is governed by the structure of the antioxidant (AgNPs) under study [60].

AgNPs of *S. platensis* was more effective on HepG2 cell line than AgNPs of *N. linckia* recording a cell viability percentage of 93% at 16 μg/ml concentration of AgNPs. The inhibitory effect was more pronounced at higher concentrations of AgNPs, leading to nearly complete mortality of the cells. This indicated that AgNP cytotoxicity on HepG2 is mainly mediated by the release of silver ions (Ag^+) from the particle surface and their consequent adsorption to the surfaces of the cells as a source of toxic Ag^+ ions, or, in the presence of oxygen, ligands, or organisms; these toxic Ag^+ ions are formed upon oxidative dissolution [61].

The AgNPs biosynthesized by *S. platensis* and *N. linckia* crude phycobiliprotein extracts attained a dose-dependent inhibition on the hepatitis C virus. The AgNPs affected viral penetration at 16 μg/ml (the pre-determined safe concentration) when added to the cells during in vitro infection, as a co-treated method [62]. *N. linckia* AgNPs recorded a higher antiviral percentage of 64.976% compared to Ribavirin (standard drug for HCV). This may be due to the smaller particle size of *N. linckia* (20.48 nm) and its lower zeta potential value ($- 16.8 \pm 6.99$ mV) compared to *S. platensis* AgNPs. These features enabled their augmentation and penetration through the virus molecules and triggered a more efficient inhibition of the viral infection activity. As it has been established, smaller AgNPs ensures a faster rate of Ag^+ distribution into the around micro-environment compared with larger sized NPs [63]. Their large surface area to volume ratio enables their higher bioavailability, augmented distribution, and consequently, their cytotoxic activity [63]. In agreement with our results, Sun et al. [64] reported that AgNPs could inhibit the replication of HIV and display promising cytoprotective activities toward HIV-infected T cells. Also, they found that AgNPs could bind to the viral particles of HIV with a regular spatial arrangement and were able to prevent the virus from binding to the host cells. El-Sheekh et al. [65] investigated both Ag_2O/AgO-NPs and Au-NPs from two blue-green algal strains, *Oscillatoria* sp. and *Spirulina platensis*, against herpes simplex virus (HSV-1). Results indicated that 90% reduction value in the cytopathic effect (CPE) of HSV-1 was achieved when applying both types of nanoparticles at 31.25-μl dose concentration, with a reduced rate of 49.23% for Ag_2O/AgO-NPs and 42.75% for Au-NPs, respectively.

5 Conclusion

The present study verified that *S. platensis* and *N. linckia* crude phycobiliprotein extract can biosynthesize AgNPs with small and stable properties. The obtained results displayed the potential antimicrobial and antioxidant capacity of these AgNPs. Moreover, the biosynthesize AgNPs exhibited potent antiviral activity against HCV and a strong cytotoxicity effect on HepG2 cell lines. The study recommended using cyanobacterial cells as commonly biological resources in the greenfield of nanotechnology for multi-purpose medicinal and pharmaceutical applications. Future studies are still in need to declare the intact cellular uptake mechanism(s) by which AgNPs exert their biological antiviral action and also to assess their safety limits for treatment, especially with human contact.

Compliance with Ethical Standards

References

1. Mohanpuria, P., Rana, N. K., & Yadav, S. K. (2008). Biosynthesis of nanoparticles: technological concepts and future applications. *Journal of Nanoparticle Research, 10*, 507–517.
2. Ismail, G. A., Allam, N. G., El-Gemizy, W. M., & Salem, M. A. (2020). The role of silver nanoparticles biosynthesized by *Anabaena variabilis* and *Spirulina platensis* cyanobacteria for malachite green removal from wastewater. *Environmental Technology.* https://doi.org/10.1080/09593330.2020.1766576.
3. Naz, M., Nasiri, N., Ikram, M., Nafees, M., Qureshi, M. Z., & Ali, S. (2017). Eco-friendly biosynthesis, anticancer drug loading and cytotoxic effect of capped Ag-nanoparticles against breast cancer. *Applied Nanoscience, 7*, 793–802.
4. Vedelago, J., Gomez, C. G., Valente, M., & Mattea, F. (2018). Green synthesis of silver nanoparticles aimed at improving theranostics. *Radiation Physics and Chemistry, 146*, 55–67.
5. Lakshmanan, G., Sathiyaseelan, A., Kalaichelvan, P. T., & Murugesan, K. (2018). Plant-mediated synthesis of silver nanoparticles using fruit extract of *Cleome viscosa* L., assessment of their antibacterial and anticancer activity. *Karbala Int J Modern Sci, 4*, 61–68.
6. Ahmed, S., Ahmad, M., Swami, B. L., & Ikram, S. (2016). A review on plants extract mediated synthesis of silver nanoparticles for antimicrobial applications, a green expertise. *Journal of Advanced Research, 7*, 17–28.
7. Balasooriya, E. R., Jayasinghe, C. D., Jayawardena, U. A., Ruwanthika, R. W. D., Mendis de Silva, R., & Udagama, R. V. (2017). Honey mediated green synthesis of nanoparticles, New era of safe nanotechnology. *J Nanomedicin* 10 pages.
8. Lee, S. H., & Jun, B. H. (2019). Silver nanoparticles, synthesis and application for nanomedicine. *Intl J Molocular Sci, 20*, 865–885.
9. Ahmed, E. A., Abdel-Hafez, E. H., Ismail, A. F. M., Elsonbaty, S. M., Abbas, H. S., & Salah El-Din, R. A. (2015). Biosynthesis of silver nanoparticles by *Spirulina platensis* and *Nostoc* sp. *Global Advanced Res J Microbiol, 4*(4), 36–49.
10. El-Sheekh, M. M., & El-Kassas, H. Y. (2016). Algal production of nano-silver and gold, their antimicrobial and cytotoxic activities, a review. *Journal, Genetic Engineering & Biotechnology, 14*, 299–310.

11. Yilma, B., & Mitiku, A. A. (2017). Antibacterial and antioxidant activity of silver nanoparticles synthesized using aqueous extract of *Moringa stenopetala* leaves. *African Journal of Biotechnology, 16*(32), 1705–1716.

12. Gaikwad, S., Ingle, A., & Gade, A. (2013). Antiviral activity of myco-synthesized silver nanoparticles against herpes simplex virus and human parainfluenza virus type 3. *International Journal of Nanomedicine, 8*, 4303–4314.

13. Ge, L., Li, Q., Wang, M., Ouyang, J., Li, X., & Xing, M. M. Q. (2014). Nanosilver particles in medical applications, synthesis, performance and toxicity. *International Journal of Nanomedicine, 9*, 2399–2407.

14. Singh, L., Kruger, H. G., Glenn, E., Maguire, M., Govender, T., & Parboosing, R. (2017). The role of nanotechnology in the treatment of viral infections. *Therapeut Adv Infectious Diseases, 4*(4), 105–130.

15. El-Naggar, N. E., Hussein, M. H., & El-Sawah, A. A. (2018). Phycobiliprotein-mediated synthesis of biogenic silver nanoparticles, characterization, *in vitro* and *in vivo* assessment of anticancer activities. *J Sci Rep, 8*, 89–97.

16. Phull, A. R., Abbas, Q., Ali, A., Raza, H., Kim, S. J., Zia, M., & Haq, I. (2016). Antioxidant, cytotoxic and antimicrobial activities of green synthesized silver nanoparticles from crude extract of *Bergenia ciliata*. *Faseb J Phycol Sci, 2*(1), 31–36.

17. Madhanraj, R., Eyini, M., & Balaji, P. (2017). Antioxidant assay of gold and silver nanoparticles from edible Basidiomycetes mushroom fungi. *Free Radicals and Antioxidants, 7*(2), 137–142.

18. Lara, H. H., Garza-Trevino, E. N., & Ixtepan-Turrent, L. (2011). Silver nanoparticles are broad-spectrum bactericidal and virucidal compounds. *Journal of Nanbiotechnology, 9*, 15–30.

19. Baskaran, X., Zhang, S., Vigila, A. V. G., Parimelazhagan, T., & Muralidhara-Rao, D. (2016). Biosynthesis, characterization, and evaluation of bioactivities of leaf extract-mediated biocompatible silver nanoparticles from an early Tracheophyte, *Pteris tripartite* Sw. *International Journal of Nanomedicine, 11*, 5789–5806.

20. Lara, H. H., Ayala-Nunez, N. V., Ixtepan-Turrent, L., & Rodriguez-Padilla, C. (2010). Mode of antiviral action of silver nanoparticles against HIV-1. *Journal of Nanbiotechnology, 8*, 31–55.

21. Kailasa, S. K., Park, T. J., Rohit, J. V., & Koduru, J. R. (2019). Antimicrobial activity of silver nanoparticles. In *Nanoparticles in pharmacotherapy* (pp. 461–484). Amsterdam, The Netherlands: Elsevier.

22. Liao, C., Li, Y., & Tjong, S. C. (2019). Bactericidal and cytotoxic properties of silver nanoparticles. *International Journal of Molecular Sciences, 20*, 449.

23. Ferdous, Z., & Nemmar, A. (2020). Health impact of silver nanoparticles: a review of the biodistribution and toxicity following various routes of exposure. *International Journal of Molecular Sciences, 21*(7), 2375. Published 2020 Mar 30. https://doi.org/10.3390/ijms21072375.

24. Patra, J., Patra, A., Mahapatra, N., Thatoi, H., Das, S., & Sahu, R. (2009). Antimicrobial activity of organic solvent extracts of three marine macroalgae from Chilika Lake, Orissa, India. Malays. *Journal of Microbiology, 5*, 128–131.

25. Salehi, S., Shandiz, S. A. S., Ghanbar, F., Darvish, M. R., Ardestani, M. S., Mirzaie, A., & Jafari, M. (2016). Phytosynthesis of silver nanoparticles using *Artemisia marschalliana Sprengel* aerial part extract and assessment of their antioxidant, anticancer and antibacterial properties. *International Journal of Nanomedicine, 11*, 1835–1846.

26. Singh, R., Parihar, P., Singh, M., Bajguz, A., Kumar, J., Singh, S., Singh, V. P., & Prasad, S. M. (2017). Uncovering potential applications of cyanobacteria and algal metabolites in biology, agriculture and medicine, status and future prospects. *Frontiers in Microbiology, 8*, 5–15.

27. Singh, S., Kate, B. N., & Banerjee, U. (2005). Bioactive compounds from cyanobacteria and microalgae, an overview. *Critical Reviews in Biotechnology, 25*, 73–95.

28. Liu, Y. F., Xu, L. Z., & Chen, N. (2000). Inhibitory effect of phycocyanin from *Spirulina platensis* on the growth of human leukemia K562 cells. *Journal of Applied Phycology, 12*(2), 125.

29. Liu, Y. F., Xu, L. Z., & Zhang, C. W. (2000). The inhibition of phycocyanin from *Porphyra haitanensis* on the on the growth of human leukemia HL-60 cells. *Chinese Journal of Marine Drugs, 19*(1), 1–20.

30. Kim, T. H., Pham, X. H., Rho, W. Y., Kim, H. M., Hahm, E., Ha, Y., Son, B. S., Lee, S. H., & Jun, B. H. (2018). Ag and Ag-Au introduced silica-coated magnetic beads. *B Korean Chem Social, 39*, 250–256.

31. Zarrouk, C. (1966). Contribution à l'étude d'une cyanophycée. Influence de divers' facteurs physiques et chimiques sur la croissance et la photosynthèse de *Spirulina maxima*. (Setch et Gardner) Geitler. Ph.D. Thesis, Université de Paris, Paris, France.

32. Rippka R, Deruelles J, Waterbury J, Herdman M, & Stanier R. (1979). Generic assignments, strain histories and properties of pure cultures of cyanobacteria. J Genetic Microbiol 111, 1–61.

33. Stainer, R. Y., Kunisawa, R., Mandel, M., & Cohen-Bazire, G. (1971). Purification and properties of unicellular blue-green algae (Order Chroococcales). *Bacteriological Reviews, 35*, 171–205.

34. Jena, J., Pradhan, N., & Dash, B. P. (2013). Biosynthesis and characterization of silver nanoparticles using microalgae *Chlorococcum humicola* and its antibacterial activity. *Int J Nanomater Biostructures, 3*, 1–8.

35. Bennett, A., & Bogorad, L. (1973). Complementary chromatic adaptation in a filamentous blue-green alga. *The Journal of Cell Biology, 58*, 419–435.

36. El-Sheekh, M. M., & El-Kassas, H. Y. (2014). Application of biosynthesized silver nanoparticles against a cancer promoter cyanobacterium, *Microcystis aeruginosa*. *Asian Pacific Journal of Cancer Prevention, 15*, 6773–6779.

37. Manual, O. (1981). *The oxoid manual of culture media ingredients and other laboratory servies* (5th ed.). UK: Oxoid Manual.

38. CLSI. (2010). *Performance standards for antimicrobial susceptibility testing, Twentieth Informational Supplement, CLSI Document M100S20* (Vol. 2010). Wayne, PA: Clinical and Laboratory Standards Institute.

39. Blois, M. S. (1958). Antioxidants determination by the use of a free radical. *Natural med, 26*, 1199–1200.

40. Prieto, P., Pineda, M., & Aguilar, M. (1999). Spectrophotometric quantitative of antioxidant capacity through the formation of a phosphomolybdenum complex, specific application to the determination of vitamin E. *Analytical Biochemistry, 269*(2), 337–341.

41. Do, Q. D., Angkawijaya, A. E., Tran-Nguyen, P. L., Huynh, L. H., Soetaredjo, F. E., Ismadji, S., & Ju, Y. H. (2014). Effect of extraction solvent on total phenol content, total flavonoid content, and antioxidant activity of *Limnophila aromatica*. *Journal of Food and Drug Analysis, 22*, 296–302.

42. Posada, D., & Crandal, K. A. (1998). Model test, testing the model of DNA substitution. *Bioinformatics, 14*, 817–818.

43. Koch, K. (2004). Antivirale effekte ausgewalter ole auf behullte viren unter besondereer Berucksichtigung des Herpes simplex Virus Type 1 and 2. Ph. D. Thesis. University of Heidelberg.

44. Lohr, D., Venkov, P., & Zlatanova, J. (1995). Transcriptional regulation in the yeast Gal gene family. A complex genetic network. *Faseb. Journal., 9*, 777–787.

45. Komurian-Pradel, F., Paranhose-Baccalà, G., Sodoyer, M., Chevallier, P., Mandrand, B., Lotteu, V., & Andre, P. (2001). Quantitation of HCV RNA using real-time PCR anf fluorimetry. *Journal of Virological Methods, 95*(1–2), 111–119. https://doi.org/10.1016/s0166-0934(01)00300-7.

46. SPSS. (2006). *SPSS base 15.0*. Chicago, USA: Users guide SPSS inc..

47. Sharma, V. K., Yngard, R. A., & Lin, Y. (2009). Silver nanoparticles, green synthesis and their antimicrobial activities. *Advances in Colloid and Interface Science, 145*, 83–96.

48. Mubarak-Ali, D. M., Gopinath, V., Rameshbabu, N., & Thajuddin, N. (2012). Synthesis and characterization of Cd-S nanoparticles using C-phycoerythrin from the marine cyanobacteria. *Mater Letter Nature, 74*, 8–11.

49. Patel, V., Berthold, D., Purannik, P., & Gantar, M. (2015). Screening of cyanobacteria and microalgae for their ability to synthesize silver nanoparticles with antibacterial activity. *Biotechnol Report, 5*, 112–119.

50. Fathima, S. R., Vadivel, A., Samuthira, N., & Mirunalini, S. (2013). Antiproliferative effect of silver nanoparticles synthesized using amla on Hep2 cell line. *Asian Pacific Journal of Tropical Medicine, 6*(1), 1–10.

51. Umoren, S. A., Obot, I. B., & Gazem, Z. M. (2014). Green synthesis and characterization of silver nanoparticles using red apple (*Malus demostica*) fruit extract at room temperature. *J Mater Environ Sci, 5*, 907–914.

52. Theivasanthi, T., & Alagar, M. (2013). Konjac biomolecules assisted- rod/spherical shaped lead nano powder synthesized by electrolytic process and characterization studies. *Nanotechnol Biomed Engin, 5*, 11–19.

53. Shivaji, S., Madhu, S., & Singh, S. (2011). Extracellular synthesis of antibacterial silver nanoparticles using psychrophilic bacteria. *Processed Biochem, 49*, 830–837.

54. Emam, M., El Raey, M. A., Eisa, W. H., El-Haddad, A. E., Osman, S. M., El-Ansari, M. A., & Rabie, A. G. (2017). Green synthesis of silver nanoparticles from *Caesalpinia gilliesii* (Hook) leaves, antimicrobial activity and in vitro cytotoxic effect against BJ-1 and MCF-7 cells. *J Appl Pharmaceut Sci, 7*, 226–233.

55. Malheiros, P. S., Micheletto, Y. M. S., Silveira, N. P., & Brandelli, A. (2010). Development and characterization of phosphatidyl choline nano vesicles containing the antimicrobial peptide Nisin. *Food Research International, 43*(4), 1198–1203.

56. Aiad, M. A., Moursi, E. A., El-Dissoky, R. A., & Amer, M. M. (2014). Response of maize crop to irrigation under different rates and dose of nitrogen fertilization in the North Nile Delta region. *J Soil Sci Agricul Engin Mansoura Univ, 5*, 97–113.

57. Tang, S., & Zheng, J. (2018). Antibacterial activity of silver nanoparticles, structural effects. *Advanced Healthcare Materials, 7*, 170–1503.

58. Long, Y. M., Hu, L. G., Yan, X. T., Zhao, X. C., Zhou, Q. F., Cai, Y., & Jiang, G.-B. (2017). Surface ligand controls silver ion release of nanosilver and its antibacterial activity against *Escherichia coli*. *International Journal of Nanomedicine, 12*, 3193.

59. Kumar, S., Shukla, A., Baul, P. P., Mitra, A., & Halder, D. (2018). Biodegradable hybrid nanocomposites of chitosan/gelatin and silver nanoparticles for active food packaging applications. *Food Science & Nutrition, 16*, 178–184.

60. Lee, H. Y., Choi, Y. J., Jung, E. J., Yin, H. Q., Kwon, J. T., & Kim, J. E. (2010). Genomics-based screening of differentially expressed genes in the brains of mice exposed to silver nanoparticles via inhalation. *Journal of Nanoparticle Research, 12*, 15–67.

61. Xiu, Z. M., Ma, J., & Alvarez, P. J. J. (2011). Differential effect of common ligands and molecular oxygen on antimicrobial activity of silver nanoparticles versus silver ions. *Environmental Science & Technology, 45*, 9003–9008.

62. Hayashi, K., Hayashi, T., & Morita, N. (1993). How an extract from *Spirulina platensis* is a selective inhibitor of herpes simplex virus type 1 penetration into HeLa cells. *Phototherapy Res, 7*, 76–80.

63. Recordati, C., De Maglie, M., Bianchessi, S., Argentiere, S., Cella, C., Mattiello, S., Cubadda, F., Aureli, F., D'Amato, M., & Raggi, A. (2016). Tissue distribution and acute toxicity of silver after single intravenous administration in mice: Nano-specific and size-dependent effects. *Particle and Fibre Toxicology, 13*, 12.

64. Sun, R. W. Y., Chen, R., Chung, N. P. Y., Ho, C. M., Lin, C. L. S., & Che, C. M. (2005). Silver nanoparticles fabricated in Hepes buffer exhibit cytoprotective activities toward HIV-1 infected cells. *Chemical Communications, 6*, 5059–5061.

65. El-Sheekh, M. M., Shabaan, M. T., Hassan, L., & Morsi, H. H. (2020). Antiviral activity of algae biosynthesized silver and gold nanoparticles against herps simplex (HSV-1) virus *in vitro* using cell-line culture technique. *International Journal of Environmental Health Research*. https://doi.org/10.1080/09603123.2020.1789946.